

# UC Davis

## UC Davis Previously Published Works

### Title

Rapid Throughput Analysis Demonstrates that Chemicals with Distinct Seizurogenic Mechanisms Differentially Alter Ca<sup>2+</sup> Dynamics in Networks Formed by Hippocampal Neurons in Culture

### Permalink

<https://escholarship.org/uc/item/6x00n7fh>

### Journal

Molecular Pharmacology, 87(4)

### ISSN

0026-895X

### Authors

Cao, Zhengyu  
Zou, Xiaohan  
Cui, Yanjun  
[et al.](#)

### Publication Date

2015-04-01

### DOI

10.1124/mol.114.096701

Peer reviewed

# Rapid Throughput Analysis Demonstrates that Chemicals with Distinct Seizurogenic Mechanisms Differentially Alter $\text{Ca}^{2+}$ Dynamics in Networks Formed by Hippocampal Neurons in Culture

Zhengyu Cao, Xiaohan Zou, Yanjun Cui, Susan Hulsizer, Pamela J. Lein, Heike Wulff, and Isaac N. Pessah

State Key Laboratory of Natural Medicines and Jiangsu Provincial Key Laboratory for TCM Evaluation and Translational Development, China Pharmaceutical University, Nanjing, P.R. China (Z.C., X.Z., Y.C.); Department of Molecular Biosciences, School of Veterinary Medicine (Z.C., Y.C., S.H., P.J.L., I.N.P.) and Department of Pharmacology, School of Medicine (H.W.), University of California, Davis, California

Received November 10, 2014; accepted January 12, 2015

## ABSTRACT

Primary cultured hippocampal neurons (HN) form functional networks displaying synchronous  $\text{Ca}^{2+}$  oscillations (SCOs) whose patterns influence plasticity. Whether chemicals with distinct seizurogenic mechanisms differentially alter SCO patterns was investigated using mouse HN loaded with the  $\text{Ca}^{2+}$  indicator fluo-4-AM. Intracellular  $\text{Ca}^{2+}$  dynamics were recorded from 96 wells simultaneously in real-time using fluorescent imaging plate reader. Although quiescent at 4 days in vitro (DIV), HN acquired distinctive SCO patterns as they matured to form extensive dendritic networks by 16 DIV. Challenge with kainate, a kainate receptor (KAR) agonist, 4-aminopyridine (4-AP), a  $\text{K}^+$  channel blocker, or pilocarpine, a muscarinic acetylcholine receptor agonist, caused distinct changes in SCO dynamics. Kainate at  $<1 \mu\text{M}$  produced a rapid rise in baseline  $\text{Ca}^{2+}$  (Phase I response) associated with high-frequency and low-amplitude SCOs (Phase II response), whereas SCOs were completely repressed with  $>1 \mu\text{M}$  kainate.

KAR competitive antagonist CNQX [6-cyano-7-nitroquinoxaline-2,3-dione] (1–10  $\mu\text{M}$ ) normalized  $\text{Ca}^{2+}$  dynamics to the prekainate pattern. Pilocarpine lacked Phase I activity but caused a sevenfold prolongation of Phase II SCOs without altering either their frequency or amplitude, an effect normalized by atropine (0.3–1  $\mu\text{M}$ ). 4-AP (1–30  $\mu\text{M}$ ) elicited a delayed Phase I response associated with persistent high-frequency, low-amplitude SCOs, and these disturbances were mitigated by pretreatment with the  $\text{K}_{\text{Ca}}$  activator SKA-31 [naphtho[1,2-*d*]thiazol-2-ylamine]. Consistent with its antiepileptic and neuroprotective activities, nonselective voltage-gated  $\text{Na}^+$  and  $\text{Ca}^{2+}$  channel blocker lamotrigine partially resolved kainate- and pilocarpine-induced  $\text{Ca}^{2+}$  dysregulation. This rapid throughput approach can discriminate among distinct seizurogenic mechanisms that alter  $\text{Ca}^{2+}$  dynamics in neuronal networks and may be useful in screening antiepileptic drug candidates.

## Introduction

Epilepsy is a complex neurological disorder that affects approximately 50 million people worldwide. It is characterized by recurrent spontaneous seizures due to neuronal hyperexcitability and hypersynchronous neuronal firing derived from various mechanisms. Seizures can cause devastating damage to the brain, leading to cognitive impairment and increased risk of

epilepsy (Reddy and Kuruba, 2013). Despite the availability of more than 20 antiepileptic drugs, around 30% of epilepsy patients experience refractory seizures or suffer from unacceptable drug side effects such as drowsiness, behavioral changes, memory impairment, or teratogenicity (Bialer and White, 2010; Sirven et al., 2012; Bialer et al., 2013).

Recent research in the epilepsy field is moving from a primary focus on controlling seizures to address the underlying pathophysiology. In animal models of epilepsy, patterns of dysregulated  $\text{Ca}^{2+}$  dynamics have been well established (McNamara et al., 2006; Deshpande et al., 2010, 2014; Chen, 2012). Aberrant  $\text{Ca}^{2+}$  dynamics have been proposed to be a major, if not essential, contributor to seizure induction and pathophysiology (McNamara et al., 2006; Chen, 2012). However, many of these studies have primarily focused on the etiological role of intracellular  $\text{Ca}^{2+}$  overload and production

This research was supported by the CounterACT Program, National Institutes of Health Office of the Director and the National Institute of Neurological Disorders and Stroke [Grant U54-NS079202], the National Institute of Environmental Health Sciences [Grants 1R01-ES020392, 3P01-ES011269, and P42-ES04699], the National Science Foundation of China [Grant 81473539], the Jiangsu Provincial Natural Science Foundation [Grant BK20141357], and the Project Program of State Key Laboratory of Natural Medicines, China Pharmaceutical University [Grant SKLNMZZJQ201402].  
dx.doi.org/10.1124/mol.114.096701.

**ABBREVIATIONS:** 4-AP, 4-aminopyridine; ARA-C, cytosine  $\beta$ -D-arabinofuranoside; CI, confidence interval; CNQX, 6-cyano-7-nitroquinoxaline-2,3-dione; DIV, days in vitro; FLIPR, fluorescent imaging plate reader; FWHM, full width at half maximum;  $\text{GABA}_A\text{R}$ ,  $\text{GABA}_A$  receptors; HN, hippocampal neurons; KAR, kainate receptor; LTG, lamotrigine; mAChR, muscarinic acetylcholine receptor; PTX, picrotoxin; SCO, synchronous  $\text{Ca}^{2+}$  oscillation; SKA-31, naphtho[1,2-*d*]thiazol-2-ylamine; TETS, tetramethylenedisulfotetramine.

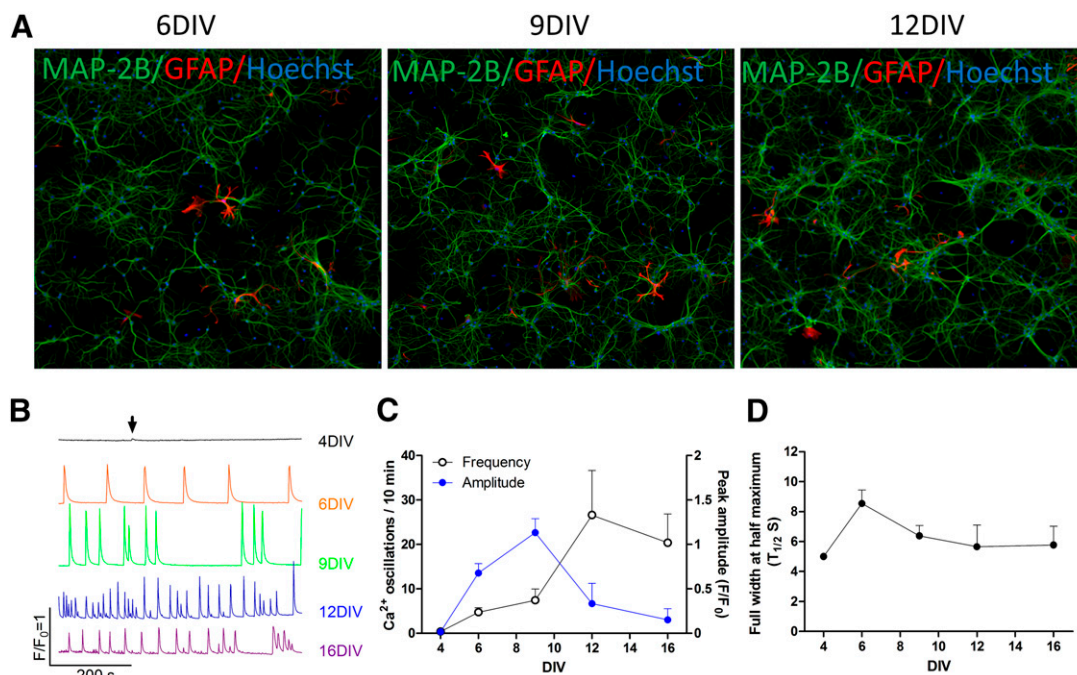


**Fig. 1.** Patterns of SCOs at defined developmental stages of primary cultured HNs in culture. (A) Representative micrographs showing immunofluorescence staining of MAP2 and GFAP in HN cultures at 6, 9, 12 DIV. (B) Representative traces of the SCOs in HN cultures at specified DIV. (C) Quantification of the SCOs frequency and amplitude in HN cultured at specified DIV. (D) Quantification of FWHM of SCOs generated by HN cultures at specified DIV. Each data point represents mean  $\pm$  S.D. from at least 5 wells, and the experiments were repeated three times.

of reactive oxygen species and redox-mediated damage after status epilepticus.

Primary dissociated cultures of hippocampal neurons form extensive dendritic networks with functional synapses that exhibit synchronous electrical activity that drive synchronous Ca<sup>2+</sup> oscillations (SCOs) (Bacci et al., 1999; Dravid and Murray, 2004; Cao et al., 2012). These SCOs control the growth and functional maturation of the neural network in vitro by regulating Ca<sup>2+</sup>-dependent pathways that influence gene transcription, metabolism, and neuronal plasticity (West and Greenberg, 2011; Wiegert and Bading, 2011; Lamont and Weber, 2012). Recent studies have demonstrated that chemicals capable of inducing status epilepticus also alter neuronal excitability and Ca<sup>2+</sup> oscillatory dynamics in hippocampal and cortical neuronal culture models (Cao et al., 2012, 2014a; Pacico and Mingorance-Le Meur, 2014). 4-Aminopyridine (4-AP), a nonselective K<sup>+</sup> channel blocker, was shown to trigger high-frequency SCOs in neocortical neurons, whereas tetramethylenedisulfotetramine (TETS) or picrotoxin, inhibitors of type A  $\gamma$ -aminobutyric acid (GABA) receptors, both produced identical temporal changes in Ca<sup>2+</sup> dynamics that included a rapid rise of baseline Ca<sup>2+</sup> (termed the Phase I response) in association with a prolonged low-frequency large-amplitude SCO pattern (termed the Phase II response) in hippocampal neurons but not in neocortical neurons (Cao et al., 2012). These recent data suggest that excitotoxic chemicals that promote seizures by engaging distinct biochemical targets might be resolved by how they differentially influence neuronal Ca<sup>2+</sup> dynamics and SCO. Importantly, acute alterations in SCO patterns could provide valuable leads to identify downstream signaling mechanisms that affect long-term changes in neuronal development and neuropathology (Cao et al., 2014b).

In this study, we investigated whether seizurogenic chemicals with distinct primary mechanisms of excitotoxicity differentially alter Ca<sup>2+</sup> dynamics and patterns of SCOs in primary hippocampal neurons (HN) that display mature neuronal network activity. The novelty to the approach was to measure changes in SCO activity before and after acute challenge of neurons loaded with Ca<sup>2+</sup> indicator fluo-4-AM while continuously monitoring intracellular Ca<sup>2+</sup> dynamics simultaneously from 96 wells in real-time using a fluorescent imaging plate reader (FLIPR). We report that epileptogenic compounds having known primary excitotoxic etiologies produce distinctive alterations in Ca<sup>2+</sup> dynamics, especially modified patterns of SCOs, which can be resolved using FLIPR. We further demonstrate the potential value of the rapid throughput assay in resolving and identifying antiepileptic drug candidates.

## Materials and Methods

Fetal bovine serum and soybean trypsin inhibitor were obtained from Atlanta Biologicals (Norcross, GA). DNase, poly-L-lysine, cytosine  $\beta$ -D-arabinofuranoside (ARA-C), kainate, 4-aminopyridine (4-AP), 6-cyano-7-nitroquinoxaline-2,3-dione (CNQX), pilocarpine, lamotrigine, and atropine were from Sigma-Aldrich (St. Louis, MO). The anti-MAP2 antibody was from Synaptic Systems (Goettingen, Germany), and the anti-GFAP antibody was from Cell Signaling Technology (Danvers, MA). The Ca<sup>2+</sup> fluorescence dye Fluo-4 and Neurobasal medium were purchased from Life Technology (Grand Island, NY). SKA-31 [naphtho [1,2-*d*]thiazol-2-ylamine] was synthesized as described previously (Sankaranarayanan et al., 2009).

**Primary Cultures of Hippocampal Neurons.** Animals were treated humanely and with regard for alleviation of suffering according to protocols approved by the Institutional Animal Care and Use Committee of the University of California, Davis. Dissociated HN with minimal astrocyte composition were cultured as described previously

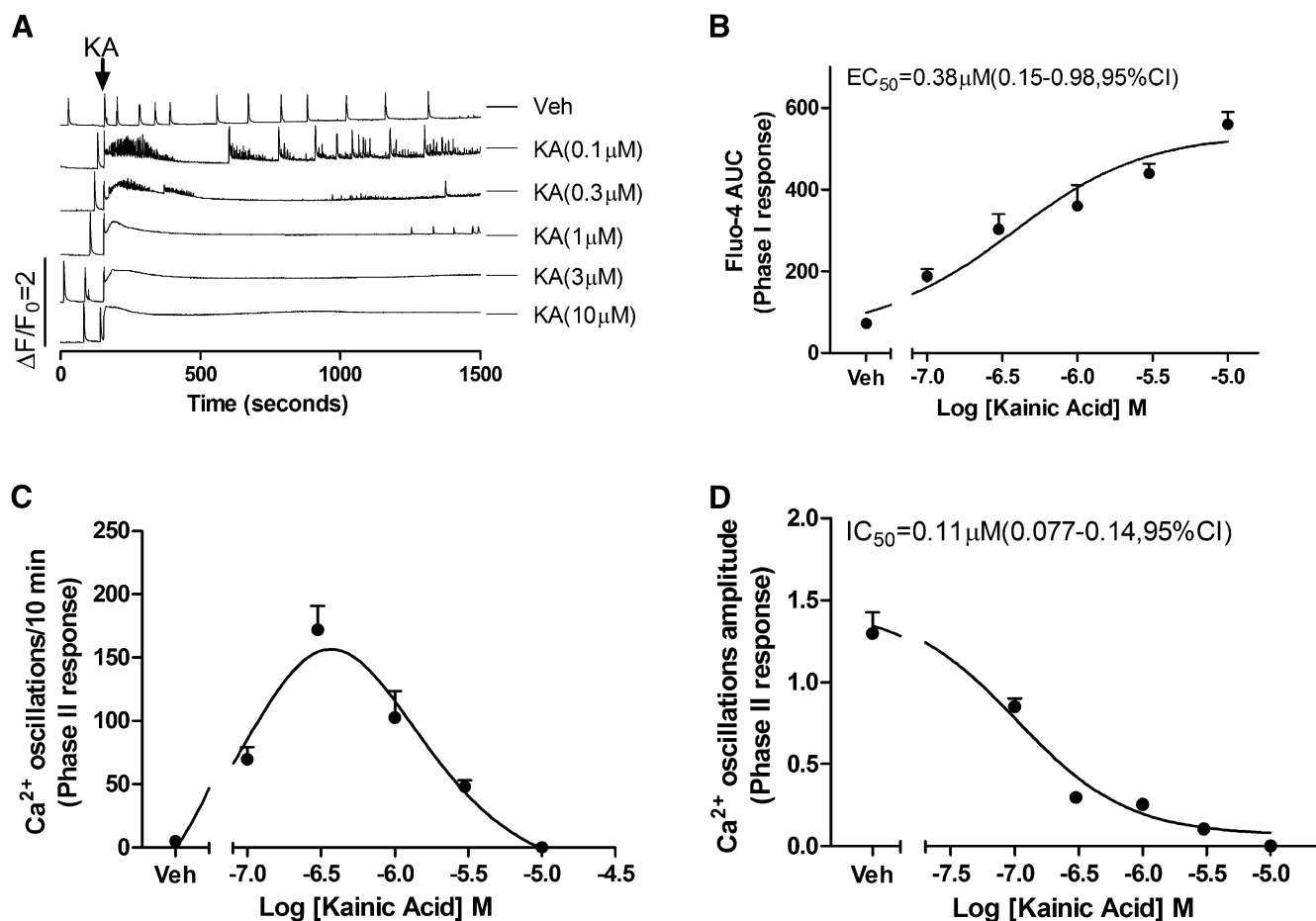


**Fig. 2.** Kainate (KA) challenge rapidly alters  $\text{Ca}^{2+}$  dynamics in 11 DIV HN cultures. (A) Representative traces of KA-induced alterations in  $\text{Ca}^{2+}$  dynamics in 11 DIV HN. KA produced an immediate intracellular  $\text{Ca}^{2+}$  rise (Phase I) and a subsequent high-frequency, low-amplitude pattern of SCOs (Phase II). The integrated  $\text{Ca}^{2+}$  phase I response (area under the curve [AUC]) was calculated from the initial 5 minutes after addition of KA to the culture medium. The phase II response was calculated from a period 10–15 minutes after addition of KA to the culture medium. (B) KA-triggered Phase I  $\text{Ca}^{2+}$  response was concentration dependent with an  $EC_{50}$  value of  $0.38 \mu\text{M}$  ( $0.15\text{--}0.8 \mu\text{M}$ , 95% CI). (C) KA induced a biphasic response on the SCOs frequency. (D) KA caused a concentration-dependent decrease on the mean amplitude of the SCOs with an  $IC_{50}$  value of  $0.11 \mu\text{M}$  ( $0.077\text{--}0.14 \mu\text{M}$ , 95% CI). Each data point represents at least four replicates, and the experiments were repeated in two independent cultures with similar results. Veh, vehicle.

(Cao et al., 2012). Briefly, neurons were dissociated from hippocampi dissected from C57BL/6J mouse pups at postnatal day 0–1 and maintained in Neurobasal complete medium [Neurobasal medium supplemented with NS21, 0.5 mM L-glutamine, HEPES (Chen et al., 2010)] with 5% fetal bovine serum. Dissociated hippocampal cells were plated onto poly-L-lysine (0.5 mg/ml)-coated clear-bottom, black wall, 96-well imaging plates (BD Biosciences, Franklin Lakes, NJ) at a density of  $0.75 \times 10^5/\text{well}$ . After 24- to 48-hour culture, a final concentration of  $10 \mu\text{M}$  ARA-C was added to the culture medium to prevent astrocyte proliferation. The medium was changed twice a week by replacing half the volume of culture medium with serum-free Neurobasal complete medium lacking fetal bovine serum. The neurons were maintained at  $37^\circ\text{C}$  with 5%  $\text{CO}_2$  and 95% humidity and measured for SCO activity at 4, 6, 9, 12, or 16 days in vitro (DIV).

**Measurement of Synchronous  $\text{Ca}^{2+}$  Oscillations.** HN were used to investigate the basal characteristics of SCOs and how seizurogenic agents alter synchronous  $\text{Ca}^{2+}$  oscillations. This method permits simultaneous measurements of intracellular  $\text{Ca}^{2+}$  transients in intact neurons in a 96-well format as described previously (Cao et al., 2010, 2012). Briefly, the growth medium was removed and replaced with dye loading buffer (100  $\mu\text{l}/\text{well}$ ) containing  $4 \mu\text{M}$  Fluo-4 and 0.5% bovine serum albumin in Locke's buffer consisting of (in mM) 4-(2-hydroxyethyl)-1-piperazineethanesulfonic acid (8.6), KCl (5.6), NaCl (154), glucose (5.6),  $\text{MgCl}_2$  (1.0),  $\text{CaCl}_2$  (2.3), and glycine (0.1), pH 7.4.

After 1 hour incubation in dye loading buffer, the neurons were washed four times in fresh Locke's buffer (200  $\mu\text{l}/\text{well}$ ) and transferred to a fluorescence laser plate reader (FLIPR Tetra; Molecular Devices, Sunnyvale, CA) incubation chamber. Baseline recording were acquired in Locke's buffer for 2–5 min followed by addition of vehicle or seizurogenic chemicals using a programmable 96-channel pipetting robotic system, and the fluorescent signals were recorded for at least an additional 30 minutes from a population of neurons at a central rectangle region of each well. Although FLIPR can record the signals at a maximum speed of 8 Hz, however, at this recording speed, the fluorescence signals decrease dramatically. The duration of a typical SCO during the basal period was 10–12 seconds depending on the development stage of the HNs. SCO data were recorded at 1 Hz, which was sufficient to resolve these events. To measure kainate- and 4-AP-stimulated SCO properties, data acquisition was increased to 2 Hz (i.e., 0.5 seconds per data point), which was sufficient to resolve SCO signal whose mean duration was approximately 4 seconds. All pharmacological interventions were performed on mature HN cultures between 9 and 12 DIV by adding the inhibitors/activators 5 or 10 minutes before addition of the seizurogenic agent. The background fluorescence of the plate was determined from a sister well without Fluo-4 loading, and all the fluorescence signals were corrected by subtracting the plate background fluorescence. Data were presented as  $F/F_0$ . The SCO frequency and amplitude were manually counted before

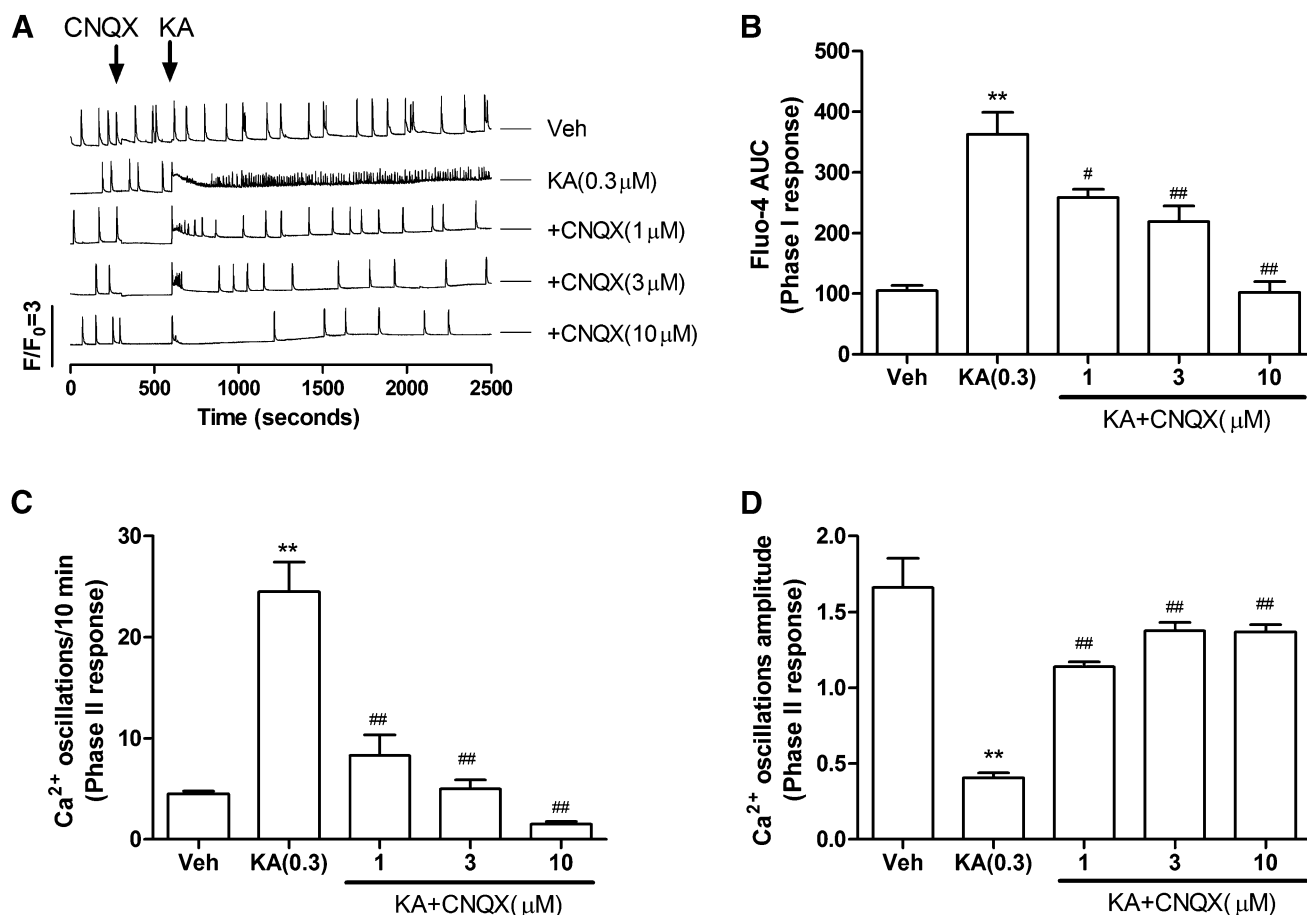


**Fig. 3.** CNQX normalized KA-induced Ca<sup>2+</sup> response in 9 DIV HN cultures. (A) Representative traces for CNQX action on KA-induced Ca<sup>2+</sup> responses. (B) CNQX ameliorated KA-induced acute Phase I Ca<sup>2+</sup> responses in a concentration-dependent manner. AUC, area under the curve. (C) CNQX suppressed KA-induced Phase II responses by increasing the frequency of Ca<sup>2+</sup> oscillations. (D) CNQX also reversed KA-induced decreases in the amplitude of Ca<sup>2+</sup> oscillations. Each data point represents at least four replicates, and the experiments were repeated twice in independent cultures with similar results. \*\**P* < 0.01, KA versus Veh (vehicle); #*P* < 0.05; ##*P* < 0.01, CNQX+KA versus KA.

and after addition of the agonists/antagonists. Events having  $F/F_0 > 0.05$  units were included in the analyses of SCO frequency and amplitude.

**Immunocytochemistry.** HN at 6, 9, and 12 DIV were fixed with 4% paraformaldehyde for 20 minutes and then permeabilized with 0.25% Triton X-100 for 15 minutes. After blocking with PBS with 10% bovine serum albumin and 1% goat serum for 1 hour, cells were incubated with anti-MAP2 (1:1000) and anti-GFAP (1:500) antibodies in PBS containing 1% goat serum overnight at 4°C. Cells were then incubated with Alexa Fluor-488-conjugated goat anti-guinea pig (1:500) and Alexa Fluor-568-conjugated goat anti-mouse (1:500) secondary antibodies for 1 hour at room temperature. After aspiration of the secondary antibody, 0.2 mg/ml Hoechst 33342 was added to each well for 5 minutes to stain the nuclei. Pictures were recorded using an ImageXpress High Content Imaging System (Molecular Devices, Sunnyvale, CA) using a 10× objective with diamidino-2-phenylindole, fluorescein isothiocyanate, and Texas Red filters. Nine adjacent sites (3 × 3), which cover ~60% of the center surface area, were imaged for each well.

**Data Analysis.** Graphing and statistical analysis were performed using GraphPad Prism software (Version 5.0; GraphPad Software Inc., San Diego, CA). The EC<sub>50</sub> and 95% confidence interval were determined by non-linear regression using GraphPad Prism software. Statistical significance between different groups was calculated using an analysis of variance and, where appropriate, a Dunnett's multiple comparison test; *P* values below 0.05 were considered statistically significant.

## Results

**Developmental Changes of SCOs in Hippocampal Neuron Cultures.** Hippocampal neurons were cultured in 96-well plates (initial density of 75,000 cells/well), and the neuronal marker MAP2 was used to stain and visualize cells at 6, 9, and 12 DIV. HN showed extensive dendritic networks by 6 DIV that increased in their complexity with age in culture (Fig. 1A, green stain). The addition of ARA-C 24- to 48-hours postplating limited the percentage of astrocytes in HN cultures detected with GFAP to less than 5% throughout the culture period investigated (Fig. 1A, red stain).

HN cultures displayed a distinctive pattern of spontaneous SCOs during the developmental window investigated (4–16 DIV). Cultures at 4 DIV displayed rare spontaneous SCOs with very small amplitude (Fig. 1B, arrow). By 6 DIV, SCOs became pronounced and displayed regular periodicity and similar amplitudes across the experiment lasting at least 10 minutes (Fig. 1B, second trace and Fig. 1C). The mean duration of each SCO, calculated as full width at half maximum (FWHM,  $T_{1/2}$ ) was significantly increased from 5 seconds at 4 DIV to  $8.5 \pm 0.9$  seconds at 6 DIV (mean  $\pm$  S.D.) (Fig. 1D). At 9 DIV, average SCO amplitude continued to increase, and although their frequency only slightly increased, the temporal pattern of SCOs became more complex with increased clustering of

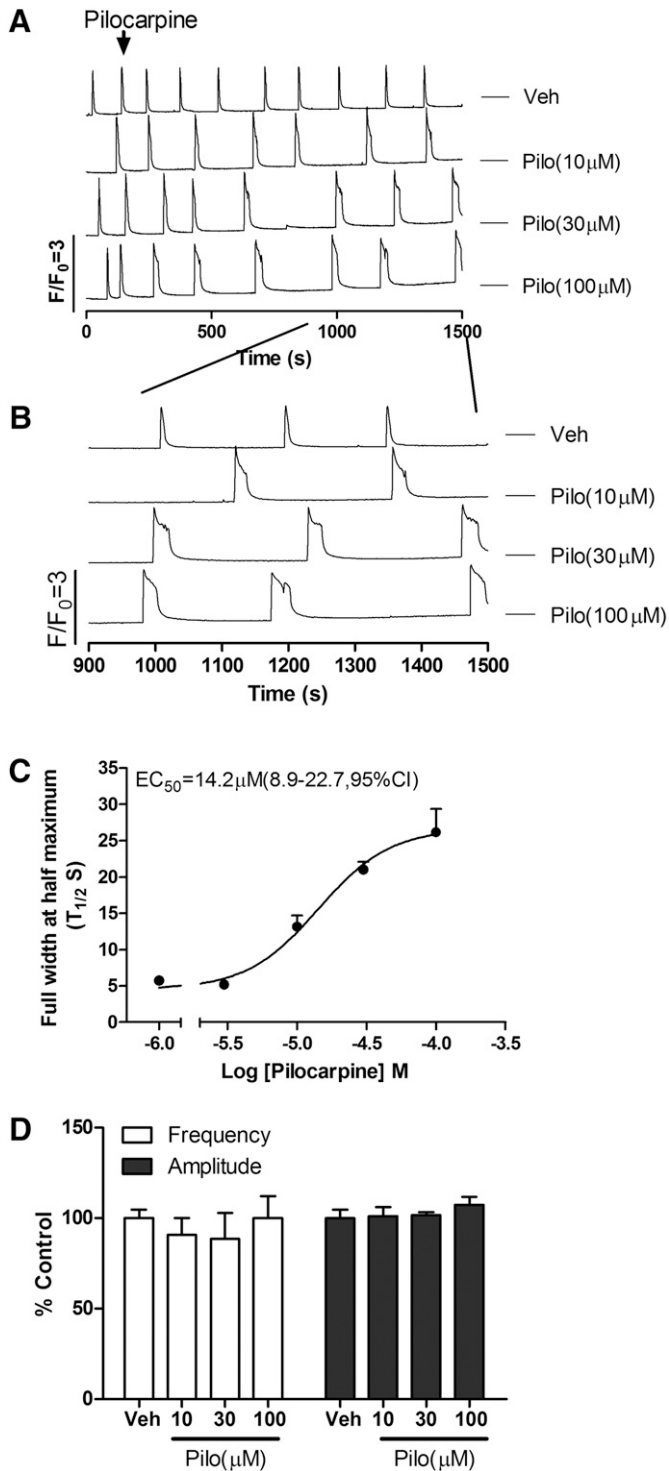


**Fig. 4.** Pilocarpine (Pilo) elicited unique modification of SCO properties in 9 DIV HN cultures. (A) Representative traces of pilocarpine-induced Ca<sup>2+</sup> responses as a function of time in 9 DIV HN cultures. Although pilocarpine did not elicit a Phase I response, it significantly prolonged SCO full width at half maximum in cultured HN. (B) Expanded traces representative of pilocarpine-induced Phase II Ca<sup>2+</sup> responses. (C) Concentration-response relationship for pilocarpine-induced prolongation of SCOs (calculated from FWHM of the SCOs). (D) Pilocarpine had no effect on the SCOs frequency and amplitude. Each data point represents at least four replicates and the experiments were repeated in three independent cultures with similar results. Veh, vehicle.

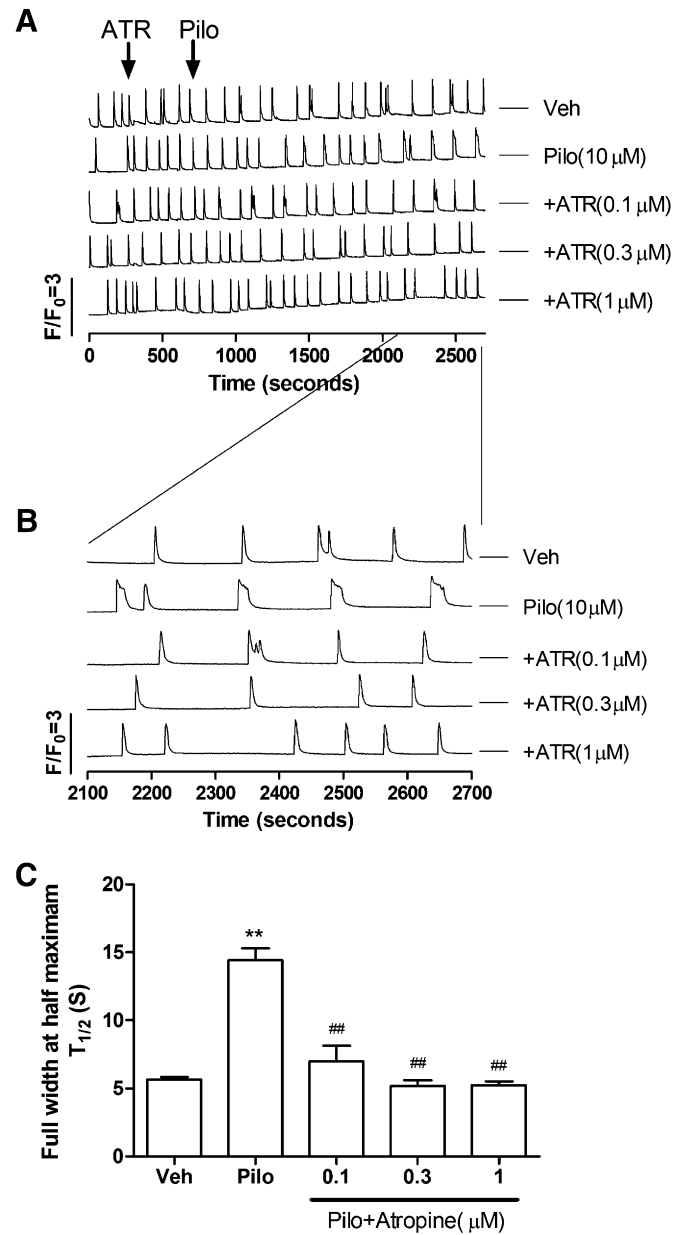


**Fig. 5.** Atropine normalized pilocarpine (Pilo; 10 µM)-induced Ca<sup>2+</sup> response in 9 DIV HN cultures. (A) Representative traces showing atropine's action on pilocarpine-induced Ca<sup>2+</sup> responses. (B) Expanded representative traces showing atropine's action on pilocarpine-induced Ca<sup>2+</sup> responses. (C) Atropine reversed pilocarpine-induced prolongation of SCO lifetime. Each data point represents at least three replicates and the experiments were repeated twice in independent cultures with similar results. \*\**P* < 0.01, pilocarpine versus Veh (vehicle); ##*P* < 0.01, pilocarpine +atropine versus pilocarpine.

events (Fig 1B, third trace). The FWHM declined to 6.4 ± 0.7 seconds (Fig 1D). By 12 DIV, SCO frequency continued to increase with each event having smaller but more heterogeneous amplitudes and increased complexity in temporal patterning (Fig. 1B, fourth trace). Thus, as the neuronal network gained morphological complexity (Fig. 1A), SCO patterning also gained temporal complexity (Fig. 1, B and C). It should be noted that although individual cultures displayed similar developmental profiles, developmental variations in SCO amplitudes and frequency were observed among the

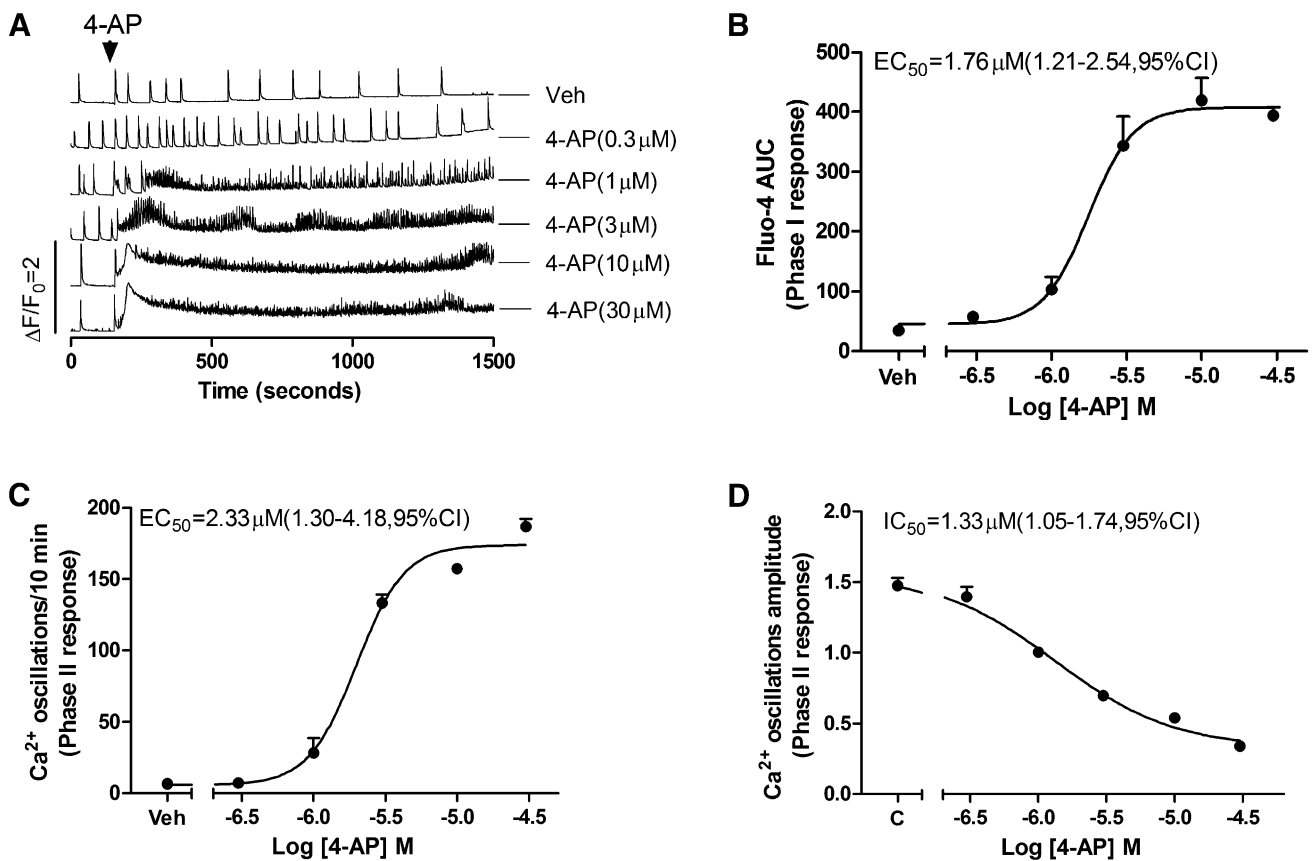


**Fig. 6.** 4-AP alters Ca<sup>2+</sup> dynamics and SCO in 10 DIV HN cultures. (A) Representative traces of 4-AP-triggered Ca<sup>2+</sup> responses in HN cultures at 10 DIV. 4-AP produced an immediate intracellular Ca<sup>2+</sup> rise (Phase I) and concomitant high frequent SCO patterns of low amplitude (Phase II). The integrated Ca<sup>2+</sup> signals (Phase I responses, area under the curve [AUC]) were calculated from the initial 5 minutes after addition of 4-AP. The Phase II responses were calculated from the 5-minute period between 10 and 15 minutes after addition of 4-AP. (B) 4-AP caused an acute concentration-dependent rise in cytoplasmic Ca<sup>2+</sup> with an EC<sub>50</sub> value of 1.76 μM (1.21–4.54 μM, 95% CI). (C) 4-AP increased SCO frequency with an EC<sub>50</sub> value of 2.33 μM (1.30–4.18 μM, 95% CI). (D) 4-AP elicited a concentration-dependent decrease in mean SCO amplitude with an IC<sub>50</sub> value of 1.33 μM (1.05–1.74 μM, 95% CI). Each data point represents at least four replicates, and the experiments were repeated in two independent cultures with similar results. Veh, vehicle.

three independent cultures assessed in this study. Nevertheless, independent cultures showed consistent developmental patterns in SCO properties and served as their own baseline for comparison to subsequent pharmacological intervention.

**Kainate Alters Ca<sup>2+</sup> Dynamics and SCO Patterns of HN Networks.** Kainate receptors (KAR) are ionotropic glutamate receptors selectively permeable to Na<sup>+</sup> and K<sup>+</sup> ions and are responsible for generating postsynaptic excitatory potentials. Although permeability to Ca<sup>2+</sup> ions is usually small, it varies with subunit composition, and their slow activation and deactivation kinetics promote appreciable Ca<sup>2+</sup> flux into postsynaptic neurons through NMDA receptor activation. The selective KAR agonist kainate is a naturally occurring excitatory amino acid commonly used in epilepsy research to induce seizures (Larsen and Bunch, 2011; Levesque and Avoli, 2013). After baseline recordings were completed, acute challenge of HN with a low concentration (0.1 μM) of kainate produced a rapid rise in baseline cytoplasmic Ca<sup>2+</sup> (termed a Phase I response) whose magnitude was concentration dependent and did not return to the prechallenge baseline for the length (20 minutes) of the recording (Fig. 2A). The EC<sub>50</sub> value for the kainate-induced Phase I response was 0.38 μM (95% confidence interval [CI], 0.15 to 0.98 μM) (Fig. 2B). Acute challenge with low concentrations of kainate (≤0.3 μM) also

elicited a short-lived burst of high-frequency SCO activity >10-fold of the initial basal activity that faded with time (termed Phase II response) (Fig. 2A, traces 2 and 3), although kainate concentrations ≥1 μM quickly abated SCO activity altogether but induced a long-lasting global increase in intracellular Ca<sup>2+</sup> (Fig. 2A, traces 4–6; Fig. 2, C and D). Therefore, kainate produced a bell-shaped Phase II concentration-effect relationship on SCOs frequency. Kainate also suppressed the Phase II response (SCOs amplitude) in a concentration-dependent manner with a half-maximal inhibition constant of 0.11 μM (0.08–0.14 μM, 95% CI, Fig. 2D).

To examine whether part or all of the Phase I and II responses observed with kainate are mediated by KAR, the cells were pretreated for 5 minutes with CNQX, a selective α-amino-3-hydroxy-5-methyl-4-isoxazolepropionic acid receptor/KAR antagonist, before challenge with kainate (0.3 μM) as described above. CNQX prevented the kainate-triggered Phase I response (at 10 μM) (Fig. 3, A and B), and at a concentration of 3 μM, abated the Phase II response (kainate-induced reduction in SCO frequency) (Fig. 3, A and C). CNQX pretreatment also greatly ameliorated the Phase II decrease in SCO amplitude produced by kainate (from 77 to 6.7% reduction in the original baseline amplitude) (Fig. 3D). CNQX at concentrations >1 μM also eliminated basal SCOs activity (Fig. 3A, traces 3–5, time scale 300–600 seconds).

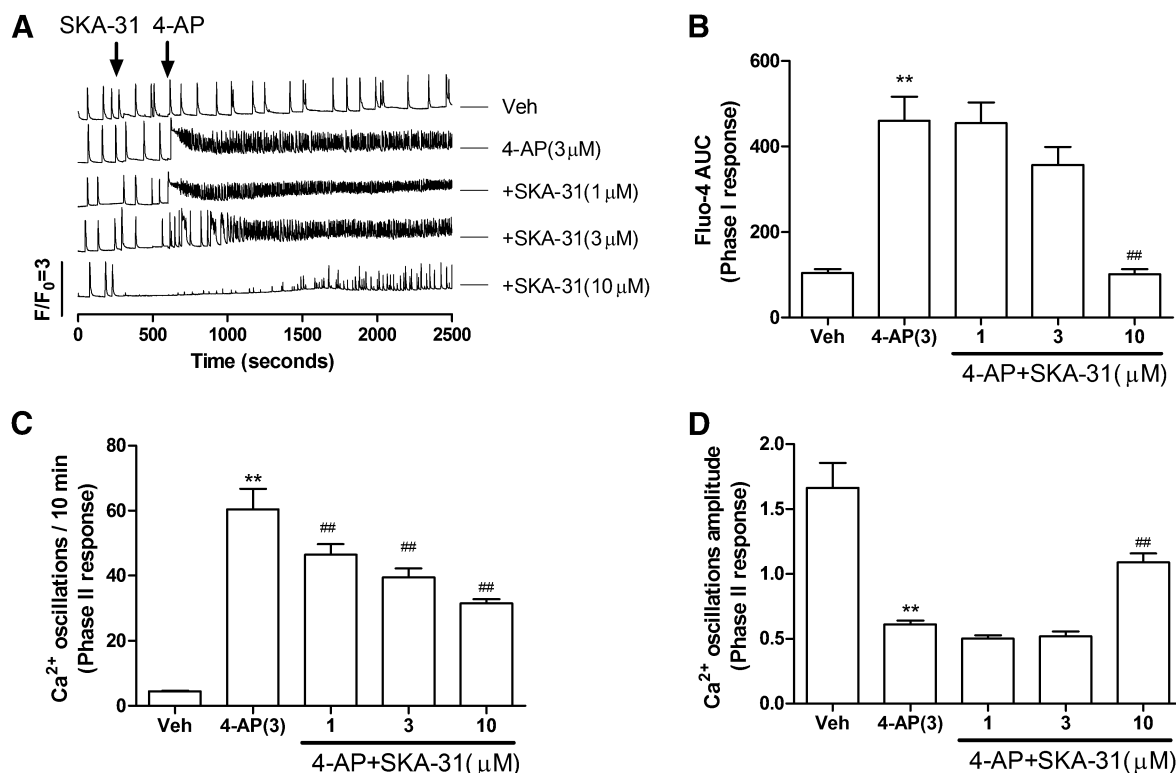


**Fig. 7.** SKA-31 normalized 4-AP (3  $\mu\text{M}$ ) triggered dysregulation of  $\text{Ca}^{2+}$  dynamics in HN cultures at 9 DIV. (A) Representative traces showing how SKA-31 influenced 4-AP-triggered  $\text{Ca}^{2+}$  dynamics. (B) SKA-31 attenuated 4-AP-induced acute rise in cytoplasmic  $\text{Ca}^{2+}$ . (C) SKA-31 attenuated 4-AP-triggered increases in SCO frequency. (D) SKA-31 attenuated 4-AP-induced decreases in SCO amplitude. Each data point represents at least three replicates, and the experiments were repeated twice in independent cultures with similar results. AUC, area under the curve. \*\* $P < 0.01$ , 4-AP versus Veh (vehicle); ### $P < 0.01$ , SKA 31+4-AP versus 4-AP.

**Pilocarpine Alters SCO Patterns in a Manner Distinct from Kainate.** Pilocarpine, a nonselective muscarinic acetylcholine receptor (mAChR) agonist, has been used to develop animal seizure models in rodents to study human epilepsy (Curia et al., 2008; de Araujo Furtado et al., 2012). Pilocarpine was chosen to investigate whether excitatory agonists that differ in their underlying mechanisms (activation of KAR versus mAChR) induce distinct SCOs responses in HN cultures. In contrast to kainate, pilocarpine (10–100  $\mu\text{M}$ ) produced a concentration- and time-dependent prolongation of SCOs (calculated as FWHM;  $T_{1/2}$ ) with an  $\text{EC}_{50}$  of 14.2  $\mu\text{M}$  (8.8–22.7  $\mu\text{M}$ , 95%CI) (Fig. 4, A–C), without affecting SCO frequencies and amplitudes (Fig. 4D). The potency is similar to pilocarpine action on the inhibition of [ $^3\text{H}$ ](R)-quinuclidinyl benzilate binding to muscarinic receptor in rat brain membranes ( $\text{IC}_{50} = 7.6 \mu\text{M}$ ) (Messer et al., 1992).

To further investigate whether HN responses to pilocarpine are primarily mediated by mAChR overactivation, the cells were pretreated with atropine, a competitive mAChR antagonist, for 10 minutes before challenge with 10  $\mu\text{M}$  pilocarpine. Atropine completely prevented pilocarpine-induced prolongation of the SCO transients (Fig. 5). Atropine itself had no significant effect on the basal SCO patterns.

**Block of Potassium Channels with 4-AP Uniquely Alters  $\text{Ca}^{2+}$  Dynamics in HN Cultures.** We next investigated the influence of a universal voltage-dependent potassium ( $\text{K}_V$ ) channel blocker 4-aminopyridine (4-AP), which has been widely used as an in vivo and in vitro model of epilepsy (Avoli et al., 2002; Kobayashi et al., 2008). Our goal was to

determine if yet another mode of action leading to excitation (inhibition of  $\text{K}_V$  currents) produced SCO patterns different from those observed in cultured HN treated with kainate or pilocarpine.

Interestingly, 4-AP (>1  $\mu\text{M}$ ) produced a Phase I rise in baseline  $\text{Ca}^{2+}$  whose overshoot was significantly delayed compared with that produced by kainate (Fig. 6A, traces 3–6) with an  $\text{EC}_{50}$  of 1.76  $\mu\text{M}$  (1.21 to 2.54  $\mu\text{M}$ ; 95% CI). Unlike either kainate or pilocarpine, 4-AP produced a long-lasting high-frequency Phase II response with persistent high frequency (>10-fold baseline) and 3-fold lower amplitude of SCOs (Fig. 6, C and D). The  $\text{EC}_{50}$  for increased SCOs frequency was 2.33  $\mu\text{M}$  (1.30–4.18  $\mu\text{M}$ , 95% CI), and the  $\text{IC}_{50}$  value for 4-AP attenuation of SCOs amplitude was 1.33  $\mu\text{M}$  (1.05–1.74  $\mu\text{M}$ , 95% CI) (Fig. 6, C and D).

SKA-31 is an activator of  $\text{Ca}^{2+}$ -activated intermediate-conductance  $\text{KCa}3.1$  and small conductance  $\text{KCa}2$  channels, which has been shown to suppress electroshock-induced seizures and improve motor deficits in a model of ataxia (Sankaranarayanan et al., 2009; Shakkottai et al., 2011). Pretreatment of HN cultures with SKA-31 (10  $\mu\text{M}$ ) for 5 minutes normalized the Phase I response to 4-AP (3  $\mu\text{M}$ ) and partially attenuated the high-frequency response and decline in amplitude in Phase II by approximately 50% each (Fig. 7, C and D). To achieve such efficacy, SKA-31 (10  $\mu\text{M}$ ) also suppressed basal SCO activity (Fig. 7A, trace 5).

**Pharmacological Antagonism with Lamotrigine Prevents Pilocarpine- and Kainate-Triggered  $\text{Ca}^{2+}$  Dysregulation.** Next we tested whether altered  $\text{Ca}^{2+}$  dynamics



elicited by pilocarpine agonism of mAChRs in the HN culture model could be prevented by a pharmacological action not mediated by direct receptor-site competition. The antiepileptic drug lamotrigine (LTG), a low-affinity Na<sup>+</sup> channel blocker preferentially binds to the inactive state of the sodium channels with  $K_d$  values of ~10  $\mu$ M (200 times less potent than block of resting channels) (Kuo and Lu, 1997). LTG (3–10  $\mu$ M) prevented the prolonged SCO duration elicited by pilocarpine (10  $\mu$ M) in HN cultures (Fig. 8, A–C).

LTG was also effective at suppressing Phase I and Phase II responses triggered by kainate (0.3  $\mu$ M); however, much higher LTG concentrations were needed (30–100  $\mu$ M), levels that also completely blocked baseline SCO activity (Fig. 9, A–D).

## Discussion

Real-time multicellular imaging of Ca<sup>2+</sup> dynamics in neuronal cultures that have established a high degree of synaptic connectivity provides a medium to high throughput in vitro approach for understanding how excitotoxicants of known mechanisms influence network connectivity at the level of local circuits. The major finding here is that distinct seizurogenic mechanisms differentially alter patterns of SCO activity measured in primary hippocampal neuronal circuits. As HN developed more complex morphology in vitro, the temporal pattern and amplitude of SCOs also became more complex. SCOs in cultured neuronal networks are dependent on action potentials and the release of synaptic neurotransmitter vesicles (Dravid and Murray, 2004). A number of studies have suggested that SCO activity is highly dependent on the balance of ongoing excitatory ionotropic glutamatergic and inhibitory GABAergic neurotransmission within the neuronal network (Dravid and Murray, 2004; George et al., 2009; Koga et al., 2010; Pacico and Mingorance-Le Meur, 2014). In addition to ionotropic Glu receptors, both type I and type II metabotropic Glu receptors also modulate SCO patterns (Dravid and Murray, 2004; Koga et al., 2010). For example, positive allosteric modulators of GABA<sub>A</sub> receptors (GABA<sub>A</sub>R), such as diazepam or allopregnanolone, decreased SCO amplitude and frequency and acted synergistically (Cao et al., 2012). In contrast, suppression of GABA<sub>A</sub> receptor function with picrotoxin (PTX), bicuculline, or tetramethylethylammonium (TETS) evoked characteristic Phase I (rapid elevation of cytosolic Ca<sup>2+</sup> level) and Phase II responses (decreased SCO frequency and increased SCO amplitude) (Cao et al., 2012). Importantly, despite the distinct molecular mechanisms by which these three chemicals interfere with GABA<sub>A</sub>R neurotransmission, they modify SCO patterns in an indistinguishable manner that differs from the excitotoxicants tested here (KA, 4-AP, pilocarpine) that target distinct receptor classes.

Although KA produced a prominent Phase I response at the lowest concentration tested (0.1  $\mu$ M), it was associated with high-frequency bursts of SCO having reduced amplitudes that eventually failed. In marked contrast to TETS, higher concentrations of KA expedited SCO failure while maintaining chronically elevated cytoplasmic Ca<sup>2+</sup>. The different patterns of Ca<sup>2+</sup> dysregulation seen with KA undoubtedly stem from the enhanced Ca<sup>2+</sup> entry mediated by prolonged activation of ionotropic GluR signaling compared with the indirect influence of impaired inhibitory inputs on Glu neurotransmission mediated by TETS (Cao et al., 2012). The observation that

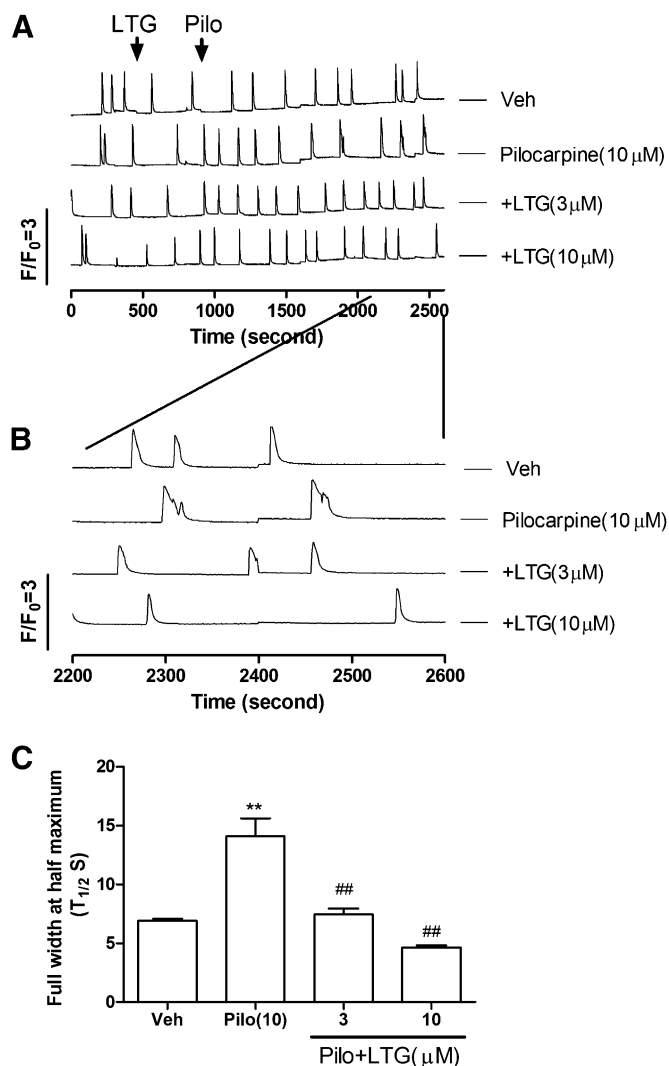


**Fig. 8.** Lamotrigine normalized pilocarpine (Pilo; 10  $\mu$ M)-induced Ca<sup>2+</sup> response in 9 DIV HN cultures. (A) Representative traces showing the actions of LTG on pilocarpine-induced Ca<sup>2+</sup> dynamics. (B) Expanded traces showing LTG actions on pilocarpine-induced Ca<sup>2+</sup> responses. (C) LTG reversed the pilocarpine-induced prolongation of SCO lifetime. Each data point represents at least three replicates, and the experiments were repeated twice in independent cultures with similar results. \*\* $P < 0.01$ , pilocarpine versus Veh (vehicle); ## $P < 0.01$ , pilocarpine+LTG versus pilocarpine.

CNQX ameliorates KA-induced Ca<sup>2+</sup> dysregulation supports our interpretation. The SCOs in primary cultured neurons are dependent on Ca<sup>2+</sup> release from intracellular Ca<sup>2+</sup> stores. Thapsigargin, which depletes Ca<sup>2+</sup> stores, suppresses SCOs in primary cultured neurons, and inhibition of 1,4,5-inositol trisphosphate receptors completely abrogated Ca<sup>2+</sup> oscillations (Dravid and Murray, 2004). KA produced a persistent Ca<sup>2+</sup> rise that stems from both Ca<sup>2+</sup> entry and Ca<sup>2+</sup> release from intracellular Ca<sup>2+</sup> stores, likely to rapidly deplete the latter (Kocsis et al., 1993; Lee et al., 2000). The loss of dynamic regulation between Ca<sup>2+</sup> entry and Ca<sup>2+</sup> stores could explain the rapid loss of SCOs in HN exposed to KA.

It further follows that nonselective K<sup>+</sup> channel negative modifiers, including 4-AP, should enhance neuronal excitability and alter Ca<sup>2+</sup> dynamics in concert (Cao et al., 2014a; Pacico and Mingorance-Le Meur, 2014). The present results

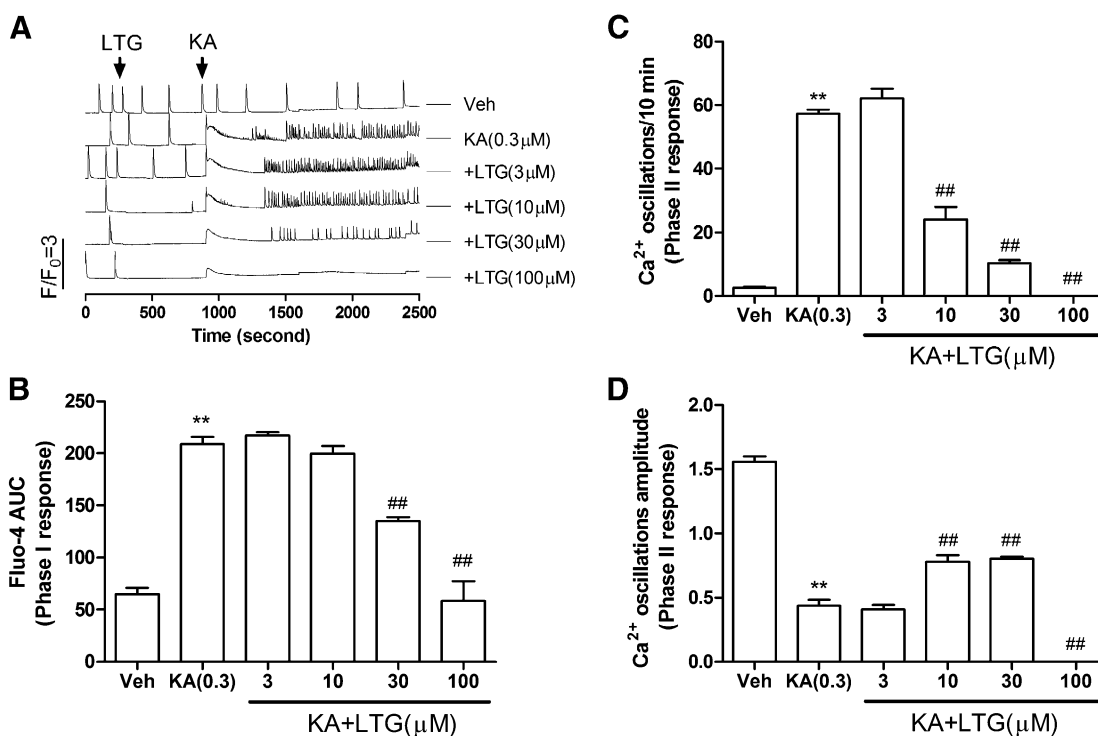


**Fig. 9.** Lamotrigine normalized KA (0.3  $\mu\text{M}$ )-induced  $\text{Ca}^{2+}$  responses in 9 DIV HN cultures. (A) Representative traces showing how LTG influences KA-induced  $\text{Ca}^{2+}$  responses. (B) LTG ameliorated KA-induced acute rise in cytoplasmic  $\text{Ca}^{2+}$  in a concentration-dependent manner. (C) LTG suppressed KA-induced increases in SCO frequency. (D) LTG also normalized KA-induced decreases SCO amplitude. Each data point represents at least three replicates, and the experiments were repeated twice in independent cultures with similar results. AUC, area under the curve. \*\* $P < 0.01$ , KA versus Veh (vehicle); ## $P < 0.01$ , LTG+KA versus 4-AP.

also reveal that in contrast to both KA and TETS (Cao et al., 2012), inhibition of  $\text{K}^+$  channels produces a delayed Phase I response that is associated with very high-frequency SCOs that persist for more than 20 minutes. SKA-31, a selective activator of  $\text{KCa}2$  and  $\text{KCa}3.1$  channels (Sankaranarayanan et al., 2009) afforded protection to 4-AP-induced  $\text{Ca}^{2+}$  dysregulation. Small- and intermediate-conductance  $\text{Ca}^{2+}$ -activated  $\text{K}^+$  channels regulate membrane potential and modulate  $\text{Ca}^{2+}$ -signaling cascades. For example,  $\text{KCa}2$  channels underlie the apamin-sensitive medium afterhyperpolarization currents and thereby regulate neuronal firing frequency and neurotransmitter release (Stocker, 2004; Wulff et al., 2007). Thus, in contrast to ligand-gated receptor mechanisms mediated by  $\text{GABA}_A$  block or KAR activation described above, 4-AP excites both excitatory and inhibitory pathways in the networks that lead to increased firing frequency of action potentials across the entire network that could explain the persistent high-frequency SCO activity seen in HN cultures. We recently demonstrated that SKA-19 [2-amino-6-trifluoromethylthio-benzothiazole], a dual-function  $\text{Na}_v1.2$  inhibitor and  $\text{KCa}2$  activator, normalizes 4-AP  $\text{Ca}^{2+}$  responses and protects against seizures in the various rodent models of epilepsy (Coleman et al., 2014).

In the CA3 region of adult rat hippocampal slices, pilocarpine induced both  $\theta$  rhythm and synchronous ictal discharges (Hadar et al., 2002). Although the basal SCO activity produced by HN cultures used in our studies failed to respond to challenge with atropine, exogenous addition of ACh modulated SCO behavior in a complex manner and was mediated by muscarinic receptor (mAChR) activation (data not shown). It is therefore not unexpected that the mAChR agonist pilocarpine modulated SCO activity in a unique manner that could be completely

normalized by pretreatment with atropine. Collectively these data further support the interpretation that basal SCO activity is mediated by excitatory Glu neurotransmission but can be modulated by mAChR activation. Pilocarpine could mediate significant prolongation of SCO events by activating excitatory  $\text{G}\alpha_q$  signaling (mediated by subtype 1, 3, and 5 mAChRs), activating inhibitory  $\text{G}\alpha_i$  signaling (mediated by types 2 and 4 mAChRs), or a balance of both ACh pathways (Lucas-Meunier et al., 2003; Brown, 2010). Because pilocarpine does not discriminate among mAChR subtypes, further studies are needed to resolve which pathway predominates in prolonging SCOs.

Collectively these data show that modification of  $\text{Ca}^{2+}$  dynamics and SCO patterns depends on the principal receptor-mediated mechanisms targeted by seizurogenic excitotoxicants, and each pattern of excitotoxic response can be ameliorated by pretreatment of the HN cultures with an agent that specifically antagonizes the excitotoxicant at their respective receptor target. Furthermore, we also demonstrate that the clinically used anticonvulsant lamotrigine antagonizes both kainate- and pilocarpine-induced  $\text{Ca}^{2+}$  responses at therapeutic concentrations. This is consistent with previous studies demonstrating that the low-affinity  $\text{Na}^+$  channel antagonist carbamazepine antagonized pilocarpine-induced status epilepticus (Morrisett et al., 1987) and neuronal cell death (Cunha et al., 2009). Both carbamazepine and LTG also suppress KA-triggered status epilepticus (Czuczwar et al., 1982; Wang et al., 2000) and neuronal cell death (Das et al., 2010; Halbsgut et al., 2013; Park et al., 2013).

It is tempting to suggest that differential patterns in  $\text{Ca}^{2+}$  dynamics and SCO patterns elicited by  $\text{GABA}_A$  blockers,

K<sup>+</sup> channel blockers, ionotropic GluR, or mAChR agonists could influence patterns of seizure onset and progression, and/or the extent of postseizure neuropathology. For example, TETS and PTX alter Ca<sup>2+</sup> dynamics and SCO patterns indistinguishably (Cao et al., 2012). In mice, intraperitoneal injections of TETS or PTX cause similar sequences of immobility, myoclonic body jerks, clonic seizures of the forelimbs and/or hindlimbs, tonic seizures (falling on the side followed by forelimb tonic contraction and hindlimb tonic extension), and eventually death (Zolkowska et al., 2012). Systematic TETS exposures that are not fatal produce transient gliosis (2–3 days postexposure) in both the hippocampus and cortex without evidence of cellular injury and neurodegeneration (Zolkowska et al., 2012; Vito et al., 2014). In contrast, administration of KA to rats induces a distinct progression of symptoms including staring episodes, head bobbing, numerous wet dog shakes, and isolated limbic motor seizures that increase in frequency, eventually leading to status epilepticus (Scerrati et al., 1986), which resemble the clinic features of human temporal lobe epilepsy (Ben-Ari, 1985). In vivo exposures to KA are known to rapidly induce neurodegeneration that is both persistent and progressive (Reddy and Kuruba, 2013; Bhowmik et al., 2014; Pritt et al., 2014). The pilocarpine seizure model displays distinct seizure behavior compared with TETS/PTX or KA. Systemic administration of pilocarpine progresses from staring spells, limbic gustatory automatisms, and motor limbic seizures that progressively developed into limbic status epilepticus that last for several hours. Pilocarpine-induced status epilepticus causes massive neuronal damage when examined at 24 to 72 hours (Turski et al., 1984, 1986). In the pilocarpine epileptic animal model, pretreatment with atropine has been shown to normalize pilocarpine-induced temporal lobe epilepsy as well as neuronal death (Jope et al., 1986; Morrisett et al., 1987; Curia et al., 2008).

In summary, we showed the developmental progression of SCO patterns in dissociated HN cultures can be measured with sufficient temporal resolution using 96-well parallel processing on the FLIPR platform. Our approach permits detailed analysis of how HN networks respond to acute exposure to excitotoxicants by measuring their basal cytoplasmic Ca<sup>2+</sup> concentrations, i.e., Ca<sup>2+</sup> dynamics as well as SCO patterns in real time. We discovered that seizurogenic chemicals that engage distinct receptor targets produce distinct changes in Ca<sup>2+</sup> dynamics and SCO patterns and, therefore, may serve as valuable rapid screening tool for identifying and classifying excitotoxicity of potential seizurogenic agents. Importantly, this approach is capable of high throughput discovery of anticonvulsants. The method also lends itself for studies of developmental neurotoxicants (Cao et al., 2014b) and those that promote neurodegeneration.

#### Authorship Contributions:

Participated in research design: Cao, Wulff, Pessah.

Conducted experiments: Cao, Cui, Hulsizer.

Contributed new reagents or analytic tools: Wulff.

Performed data analysis: Cao, Zou, Cui.

Wrote or contributed to the writing of the manuscript: Cao, Lein, Wulff, Pessah.

#### References

Avoli M, D'Antuono M, Louvel J, Köhling R, Biagini G, Pumain R, D'Arcangelo G, and Tancredi V (2002) Network and pharmacological mechanisms leading to epileptiform synchronization in the limbic system in vitro. *Prog Neurobiol* **68**:167–207.

Bacci A, Verderio C, Pravettoni E, and Matteoli M (1999) Synaptic and intrinsic mechanisms shape synchronous oscillations in hippocampal neurons in culture. *Eur J Neurosci* **11**:389–397.

Ben-Ari Y (1985) Limbic seizure and brain damage produced by kainic acid: mechanisms and relevance to human temporal lobe epilepsy. *Neuroscience* **14**:375–403.

Bhowmik M, Saini N, and Vohora D (2014) Histamine H3 receptor antagonism by ABT-239 attenuates kainic acid induced excitotoxicity in mice. *Brain Res* **1581**:129–140.

Bialer M, Johannessen SI, Levy RH, Perucca E, Tomson T, and White HS (2013) Progress report on new antiepileptic drugs: a summary of the Eleventh Eilat Conference (EILAT XI). *Epilepsia Res* **103**:2–30.

Bialer M and White HS (2010) Key factors in the discovery and development of new antiepileptic drugs. *Nat Rev Drug Discov* **9**:68–82.

Brown DA (2010) Muscarinic acetylcholine receptors (mAChRs) in the nervous system: some functions and mechanisms. *J Mol Neurosci* **41**:340–346.

Cao Z, Cui Y, Busse E, Mehrotra S, Rainier JD, and Murray TF (2014a) Gambierol inhibition of voltage-gated potassium channels augments spontaneous Ca<sup>2+</sup> oscillations in cerebrocortical neurons. *J Pharmacol Exp Ther* **350**:615–623.

Cao Z, Cui Y, Nguyen HM, Jenkins DP, Wulff H, and Pessah IN (2014b) Nanomolar bifenthrin alters synchronous Ca<sup>2+</sup> oscillations and cortical neuron development independent of sodium channel activity. *Mol Pharmacol* **85**:630–639.

Cao Z, Hammock BD, McCoy M, Rogawski MA, Lein PJ, and Pessah IN (2012) Tetramethylenedisulfotetramine alters Ca<sup>2+</sup> dynamics in cultured hippocampal neurons: mitigation by NMDA receptor blockade and GABA(A) receptor-positive modulation. *Toxicol Sci* **130**:362–372.

Cao Z, LePage KT, Frederick MO, Nicolaou KC, and Murray TF (2010) Involvement of caspase activation in azaspiricid-induced neurotoxicity in neocortical neurons. *Toxicol Sci* **114**:323–334.

Chen Y (2012) Organophosphate-induced brain damage: mechanisms, neuropsychiatric and neurological consequences, and potential therapeutic strategies. *Neurotoxicology* **33**:391–400.

Chen Y, Tassone F, Berman RF, Hagerman PJ, Hagerman RJ, Willemsen R, and Pessah IN (2010) Murine hippocampal neurons expressing Fmr1 gene pre-mutations show early developmental deficits and late degeneration. *Hum Mol Genet* **19**:196–208.

Coleman N, Nguyen HM, Cao Z, Brown BM, Jenkins DP, Zolkowska D, Chen YJ, Tanaka BS, and Goldin AL et al. (2014). The riluzole derivative 2-amino-6-trifluoromethylthio-benzothiazole (SKA-19), a mixed K2 activator and Na blocker, is a potent novel anticonvulsant. *Neurotherapeutics*, in press.

Cunha AO, Mortari MR, Liberato JL, and dos Santos WF (2009) Neuroprotective effects of diazepam, carbamazepine, phenytoin and ketamine after pilocarpine-induced status epilepticus. *Basic Clin Pharmacol Toxicol* **104**:470–477.

Curia G, Longo D, Biagini G, Jones RS, and Avoli M (2008) The pilocarpine model of temporal lobe epilepsy. *J Neurosci Methods* **172**:143–157.

Czuczwar SJ, Turski L, and Kleinrok Z (1982) Anticonvulsant action of phenobarbital, diazepam, carbamazepine, and diphenylhydantoin in the electroshock test in mice after lesion of hippocampal pyramidal cells with intracerebroventricular kainic acid. *Epilepsia* **23**:377–382.

Das A, McDowell M, O'Dell CM, Busch ME, Smith JA, Ray SK, and Banik NL (2010) Post-treatment with voltage-gated Na(+) channel blocker attenuates kainic acid-induced apoptosis in rat primary hippocampal neurons. *Neurochem Res* **35**:2175–2183.

de Araujo Furtado M, Rossetti F, Chanda S, and Yourick D (2012) Exposure to nerve agents: from status epilepticus to neuroinflammation, brain damage, neurogenesis and epilepsy. *Neurotoxicology* **33**:1476–1490.

Deshpande LS, Carter DS, Blair RE, and DeLorenzo RJ (2010) Development of a prolonged calcium plateau in hippocampal neurons in rats surviving status epilepticus induced by the organophosphate diisopropylfluorophosphate. *Toxicol Sci* **116**:623–631.

Deshpande LS, Carter DS, Phillips KF, Blair RE, and DeLorenzo RJ (2014) Development of status epilepticus, sustained calcium elevations and neuronal injury in a rat survival model of lethal paraoxon intoxication. *Neurotoxicology* **44**:17–26.

Dravid SM and Murray TF (2004) Spontaneous synchronized calcium oscillations in neocortical neurons in the presence of physiological [Mg(2+)]<sub>i</sub>: involvement of AMPA/kainate and metabotropic glutamate receptors. *Brain Res* **1006**:8–17.

George J, Dravid SM, Prakash A, Xie J, Peterson J, Jabba SV, Baden DG, and Murray TF (2009) Sodium channel activation augments NMDA receptor function and promotes neurite outgrowth in immature cerebrocortical neurons. *J Neurosci* **29**:3288–3301.

Hadar EJ, Yang Y, Sayin U, and Rutecki PA (2002) Suppression of pilocarpine-induced ictal oscillations in the hippocampal slice. *Epilepsia Res* **49**:61–71.

Halbsgut LR, Fahim E, Kapoor K, Hong H, and Friedman LK (2013) Certain secondary antiepileptic drugs can rescue hippocampal injury following a critical growth period despite poor anticonvulsant activity and cognitive deficits. *Epilepsy Behav* **29**:466–477.

Jope RS, Morrisett RA, and Snead OC (1986) Characterization of lithium potentiation of pilocarpine-induced status epilepticus in rats. *Exp Neurol* **91**:471–480.

Kobayashi K, Nishizawa Y, Sawada K, Ogura H, and Miyabe M (2008) K(+) channel openers suppress epileptiform activities induced by 4-aminopyridine in cultured rat hippocampal neurons. *J Pharmacol Sci* **108**:517–528.

Kocsis JD, Rand MN, Chen B, Waxman SG, and Pourcho R (1993) Kainate elicits elevated nuclear calcium signals in retinal neurons via calcium-induced calcium release. *Brain Res* **616**:273–282.

Koga K, Iwahori Y, Ozaki S, and Ohta H (2010) Regulation of spontaneous Ca(2+) spikes by metabotropic glutamate receptors in primary cultures of rat cortical neurons. *J Neurosci Res* **88**:2252–2262.

Kuo CC and Lu L (1997) Characterization of lamotrigine inhibition of Na<sup>+</sup> channels in rat hippocampal neurons. *Br J Pharmacol* **121**:1231–1238.

Lamont MG and Weber JT (2012) The role of calcium in synaptic plasticity and motor learning in the cerebellar cortex. *Neurosci Biobehav Rev* **36**:1153–1162.

Larsen AM and Bunch L (2011) Medicinal chemistry of competitive kainate receptor antagonists. *ACS Chem Neurosci* **2**:60–74.

Lee YH, Fang KM, Yang CM, Hwang HM, Chiu CT, and Tsai W (2000) Kainic acid-induced neurotrophic activities in developing cortical neurons. *J Neurochem* **74**:2401–2411.

- Lévesque M and Avoli M (2013) The kainic acid model of temporal lobe epilepsy. *Neurosci Biobehav Rev* **37**:2887–2899.
- Lucas-Meunier E, Fossier P, Baux G, and Amar M (2003) Cholinergic modulation of the cortical neuronal network. *Pflugers Arch* **446**:17–29.
- McNamara JO, Huang YZ, and Leonard AS (2006) Molecular signaling mechanisms underlying epileptogenesis. *Sci STKE* **2006**:re12.
- Messer WS Jr, Ngur DO, Abuh YF, Dokas LA, Ting SM, Hacksell U, Nilsson BM, Dunbar PG, and Hoss W (1992) Stereoselective binding and activity of oxotremorine analogs at muscarinic receptors in rat brain. *Chirality* **4**:463–468.
- Morrisett RA, Jope RS, and Snead OC, 3rd (1987) Effects of drugs on the initiation and maintenance of status epilepticus induced by administration of pilocarpine to lithium-pretreated rats. *Exp Neurol* **97**:193–200.
- Pacico N and Mingorance-Le Meur A (2014) New in vitro phenotypic assay for epilepsy: fluorescent measurement of synchronized neuronal calcium oscillations. *PLoS ONE* **9**:e84755.
- Park HJ, Kim SK, Chung JH, and Kim JW (2013) Protective effect of carbamazepine on kainic acid-induced neuronal cell death through activation of signal transducer and activator of transcription-3. *J Mol Neurosci* **49**:172–181.
- Pritt ML, Hall DG, Jordan WH, Ballard DW, Wang KK, Müller UR, and Watson DE (2014) Initial biological qualification of SBDP-145 as a biomarker of compound-induced neurodegeneration in the rat. *Toxicol Sci* **141**:398–408.
- Reddy DS and Kuruba R (2013) Experimental models of status epilepticus and neuronal injury for evaluation of therapeutic interventions. *Int J Mol Sci* **14**:18284–18318.
- Sankaranarayanan A, Raman G, Busch C, Schultz T, Zimin PI, Hoyer J, Köhler R, and Wulff H (2009) Naphtho[1,2-d]thiazol-2-ylamine (SKA-31), a new activator of KCa2 and KCa3.1 potassium channels, potentiates the endothelium-derived hyperpolarizing factor response and lowers blood pressure. *Mol Pharmacol* **75**:281–295.
- Scerrati M, Onofri M, Pacifici L, Pola P, Ramacci MT, and Rossi GF (1986) Electro-cerebral and behavioural analysis of systemic kainic acid-induced epilepsy in the rat. *Drugs Exp Clin Res* **12**:671–680.
- Shakkottai VG, do Carmo Costa M, Dell'Orco JM, Sankaranarayanan A, Wulff H, and Paulson HL (2011) Early changes in cerebellar physiology accompany motor dysfunction in the polyglutamine disease spinocerebellar ataxia type 3. *J Neurosci* **31**:13002–13014.
- Sirven JI, Noe K, Hoerth M, and Drazkowski J (2012) Antiepileptic drugs 2012: recent advances and trends. *Mayo Clin Proc* **87**:879–889.
- Stocker M (2004) Ca<sup>2+</sup>-activated K<sup>+</sup> channels: molecular determinants and function of the SK family. *Nat Rev Neurosci* **5**:758–770.
- Turski L, Cavalheiro EA, Sieklucka-Dziuba M, Ikonomidou-Turski C, Czuczwar SJ, and Turski WA (1986) Seizures produced by pilocarpine: neuropathological sequelae and activity of glutamate decarboxylase in the rat forebrain. *Brain Res* **398**:37–48.
- Turski WA, Cavalheiro EA, Bortolotto ZA, Mello LM, Schwarz M, and Turski L (1984) Seizures produced by pilocarpine in mice: a behavioral, electroencephalographic and morphological analysis. *Brain Res* **321**:237–253.
- Vito ST, Austin AT, Banks CN, Inceoglu B, Bruun DA, Zolkowska D, Tancredi DJ, Rogawski MA, Hammock BD, and Lein PJ (2014) Post-exposure administration of diazepam combined with soluble epoxide hydrolase inhibition stops seizures and modulates neuroinflammation in a murine model of acute TETS intoxication. *Toxicol Appl Pharmacol* **281**:185–194.
- Wang L, Zuo CH, Zhao DY, and Wu XR (2000) Brain distribution and efficacy of carbamazepine in kainic acid induced seizure in rats. *Brain Dev* **22**:154–157.
- West AE and Greenberg ME (2011) Neuronal activity-regulated gene transcription in synapse development and cognitive function. *Cold Spring Harb Perspect Biol* **3**.
- Wiegert JS and Bading H (2011) Activity-dependent calcium signaling and ERK-MAP kinases in neurons: a link to structural plasticity of the nucleus and gene transcription regulation. *Cell Calcium* **49**:296–305.
- Wulff H, Kolski-Andreaco A, Sankaranarayanan A, Sabatier JM, and Shakkottai V (2007) Modulators of small- and intermediate-conductance calcium-activated potassium channels and their therapeutic indications. *Curr Med Chem* **14**:1437–1457.
- Zolkowska D, Banks CN, Dhir A, Inceoglu B, Sanborn JR, McCoy MR, Bruun DA, Hammock BD, Lein PJ, and Rogawski MA (2012) Characterization of seizures induced by acute and repeated exposure to tetramethylenedisulfotetramine. *J Pharmacol Exp Ther* **341**:435–446.

---

**Address correspondence to:** Isaac N. Pessah, Department of Molecular Biosciences, School of Veterinary Medicine, 1089 Veterinary Medicine Drive, University of California, Davis, One Shields Avenue, Davis, CA 95616. E-mail: inpessah@ucdavis.edu

---